Journal of Materials Chemistry B

ROYAL SOCIETY OF CHEMISTRY

PAPER

Cite this: *J. Mater. Chem. B*, 2020, **8**, 2814

Non-equilibrium organosilane plasma polymerization for modulating the surface of PTFE towards potential blood contact applications†

Vineeth M. Vijayan,[ab] Bernabe S. Tucker,[b] Patrick T. J. Hwang,[c] Pratheek S. Bobba,[d] Ho-Wook Jun,[d] Shane A. Catledge,[a] Yogesh K. Vohra[a] and Vinoy Thomas *[ab]

Received 4th December 2019,
Accepted 12th February 2020

DOI: 10.1039/c9tb02757b

rsc.li/materials-b

We report a novel and facile organosilane plasma polymerization method designed to improve the surface characteristics of poly(tetrafluoroethylene) (PTFE). We hypothesized that the polymerized silane coating would provide an adhesive surface for endothelial cell proliferation due to a large number of surface hydroxyl groups, while the large polymer networks on the surface of PTFE would hinder platelet attachment. The plasma polymerized PTFE surfaces were then systematically characterized *via* different analytical techniques such as FTIR, XPS, XRD, Contact angle, and SEM. The key finding of the characterization is the time-dependent deposition of an organosilane layer on the surface of PTFE. This layer was found to provide favorable surface properties to PTFE such as a very high surface oxygen content, high hydrophilicity and improved surface mechanics. Additionally, *in vitro* cellular studies were conducted to determine the bio-interface properties of the plasma-treated and untreated PTFE. The important results of these experiments were rapid endothelial cell growth and decreased platelet attachment on the plasma-treated PTFE compared to untreated PTFE. Thus, this new surface modification technique could potentially address the current challenges associated with PTFE for blood contact applications, specifically poor endothelial cell growth and risk of thrombosis.

1. Introduction

Surface modification is one of the widely used routes to augment biomaterials for appropriate cell responses. Plasma treatment/polymerization is a facile surface modification technique for polymers that has been employed for decades.[1,2] The nondestructive and *in situ* sterilization capabilities of this technique make it an attractive candidate for modifying the surface properties of biomaterials without compromising their bulk properties. Plasma, the fourth state of matter, is composed of mixtures of ions, electrons, radicals, and neutral atoms/molecuales which upon colliding on the surface of materials can rearrange or alter their surface chemistry.[3,4] It can introduce various surface functional groups such as amino, carboxyl and hydroxyl groups on their surface.[5] These functional groups can be further conjugated with various biomolecules, growth factors or peptides for a variety of biomedical applications.[6,7] The surface properties of biomaterials are very critical for determining the proein/cellular responses which in turn will decide the success rate of implant biomaterials inside the body. Chemical surface modification is typically accomplished through performing certain surface reactions by wet chemistry.[8] This process is time consuming and can also lead to some residual chemicals over the surface. This can affect the functional performance of a material inside the body. The absence of multiple reagents that wet chemistry use for surface functionalization, thus, makes plasma treatment as a safe, alternative method for surface modification of biomaterials.[9] Plasma surface modification is a simple and robust method, and can safely and reliably modify the surface properties of biomaterials towards different biomedical applications. However, the plasma surface modification of biomaterials is typically accomplished by using conventional feed gases such as oxygen, ammonia, nitrogen and hydrogen.[10–13] These gases can introduce different functional groups such as carboxyl, amino and hydroxyl groups. However, these conventionally modified surfaces are always subject to ageing (surface reorganization); thus, ageing hinders their long-term ability to retain the material properties associated with better cellular responses.[14,15]

[a] *Center for Nanoscale Materials and Biointegration, The University of Alabama at Birmingham, Birmingham, AL 35294, USA. E-mail: vthomas@uab.edu*
[b] *Department of Material Science and Engineering, The University of Alabama at Birmingham, Birmingham, AL 35294, USA*
[c] *Endomimetics, LLC, Birmingham, Alabama, 35203, USA*
[d] *Department of Biomedical Engineering, The University of Alabama at Birmingham, Birmingham, AL 35294, USA*

† Electronic supplementary information (ESI) available. See DOI: 10.1039/c9tb02757b

Plasma has an interesting capability to induce polymerization of volatile organic monomers through a process called plasma enhanced chemical vapor deposition (PECVD); the polymers can be deposited over the surface of a substrate.[16,17] The high energy species formed as a result of this process causes a chain of reactions and, subsequently, causes the polymerization of the reactive monomers. But, unlike conventional polymers, plasma based polymers are not well organized as they have a random arrangement.[18] Recently, plasma polymerization has played a major role in tissue regeneration applications.[19] Plasma polymerization of reactive monomers can tailor the surface properties of polymeric biomaterials to endow them with favorable cellular responses. More specific examples of such recent studies are plasma polymerization of organic monomers like acrylic acid and allyl amine on polymeric biomaterials.[20–22] Results of these studies suggest that these organic monomers when plasma polymerized endow polymer biomaterials with better cell adhesion and proliferation capabilities. More importantly stability studies conducted on them, specifically on plasma polymerized acrylic acid coatings, have exhibited high stability; suggesting their potential utility for different biomedical applications.[23] Hence, plasma polymerizations of organic monomers have a wide scope to tailor the surface properties of biomaterials for different biointerface applications.

PTFE is a fluoropolymer which is widely used as a vascular graft material.[24,25] The chemically inert nature of PTFE makes it an ideal implantable material. Even though large diameter PTFE vascular grafts ($\geq$6 mm) have been reported as successful,[25] small diameter PTFE vascular grafts ($\leq$4 mm) still have serious issues.[26] Some of the important challenges associated with small diameter PTFE vascular grafts are thrombosis and lack of endothelial cell growth. The hydrophobic nature of PTFE makes it very difficult for endothelial cells to attach and grow to a confluent layer. Hence, it is essential to tailor the surface properties of PTFE to meet the requirements of small diameter vascular grafts. One of the most important methods of modifying the surface properties of PTFE is plasma modification. Different types of plasma processing are reported for modifying the surface properties of PTFE. Most of them are oxygen plasma, ammonia plasma and hydrogen plasma processing.[27–29] The major drawback of these plasma surface modification routes is ageing (a significant reduction in functional groups with time).[30] Moreover, post-processing multistep conjugations with peptides and antithrombotic agents are further needed to favor endothelial cell growth. Recently, hybrid processes (plasma modification and chemical modification) have been reported to tailor the surface properties of PTFE for blood contact applications.[31,32] These processes utilized the combination of oxygen plasma and dopamine surface functionalization for improving the endothelial cell affinity and anti-thrombogenicity. However, these types of hybrid processes require multiple chemical reagents with several steps and they are time consuming. Hence, a more efficient and facile method of surface modification of PTFE would be highly appreciated for blood contact applications. Plasma polymerizations of organic monomers are never explored to tailor the surface properties of PTFE for blood contact applications. Inspired by this idea, in the current study we explored the plasma polymerization of an organosilane precursor, more specifically tertraethoxysilane (TEOS) to modify the surface properties of PTFE for blood contact applications. We hypothesized that the plasma polymerization of TEOS will endow PTFE with favorable surface properties for potential blood contact applications. To the best of our knowledge there are no reports exploring the plasma polymerization capability of this organosilane monomer for tailoring/modifying the surface properties of PTFE for blood contact applications.

2. Materials and methods

The PTFE substrate used for the plasma modification (Laboratory grade PTFE sheets) was purchased from Oil sleek company, USA. The Harrick Plasma chamber (PDC-001-HP) used for the plasma surface modification was purchased from Harrick Plasma, New York, USA. The reagents used for the experiments such as tetraethoxysilane and acetone were purchased from Sigma Aldrich.

2.1. Plasma polymerization of tertraethoxysilane on PTFE

The PTFE sheets were cut into 3 cm $\times$ 1.2 cm (0.2 mm thickness) pieces for plasma treatment. Briefly, the samples were washed with acetone for 30 min before the plasma treatment to remove the adsorbed impurities (if any) from the surface. The PTFE samples were then placed inside a Harrick Plasma chamber (PDC-001-HP) and a radiofrequency (13.56 MHz, 45 W) was used for plasma treatment. The plasma polymerization process of TEOS was accomplished by using a combination of a TEOS-air system inside the plasma chamber. Briefly, 1 mL of TEOS was placed on a glass slide adjacent to the PTFE samples inside the chamber, followed by applying a constant Air flow rate of 50 sccm inside the chamber. The reduced pressure (500 mTorr inside the chamber) facilitates the formation of TEOS vapors. Different plasma treatment times such as 10, 20 and 30 min were employed for optimizing the plasma polymerization process. Herein they are referred to as PTFE-t10, PTFE-t20 and PTFE-t30 which correspond to 10 min, 20 min, and 30 min respectively.

2.2. Characterization

Fourier-transform infrared spectroscopy (FTIR) and X-ray photoelectron spectroscopy (XPS) were employed to elucidate the surface chemistry. The Bruker alpha FTIR spectrometer with ATR mode was used to acquire IR-absorption spectra (ranging from 4000 to 400 cm^{-1}). The XPS spectra of plasma treated samples were obtained using a Phi 5000 Versaprobe made by Phi Electronics, Inc. (Chanhassen, WI USA). The X-ray source of this instrument is a monochromatic, focused, Al K-alpha source (E = 1486.6 eV) at 25 W with a 100 micrometer spot size. A Mg anode (λ = 1253.6 eV) was used at 300 W and a barium oxide neutralizer eliminated the charging. The survey scans (4 scans averaged per analysis) were obtained using a pass energy of 187.5 eV with a step size of 0.5 eV. The high resolution scans (8 scans average per analysis) were obtained with a pass energy of 23.5 eV and a step size of 0.1 eV.

To measure the contact angle, the samples (n = 3) and were mounted onto a glass slide. Contact angles were measured using the sessile drop method as reported previously at room temperature.[33] The water droplet size was 5 μL. ImageJ software was used to accurately measure the contact angle of the water droplets on the surface.

The X-ray diffraction (XRD) experiments were performed on an Empyrean X-ray diffractometer (Malvern Panalytical, UK) equipped with a Cu LFF HR X-ray tube at 30 kV tension and 10 mA current. The spectrum was recorded in the range of 2θ from 10 to 100. The structure and morphology of the plasma treated and untreated control PTFE tape were characterized by scanning electron microscopy (SEM) after sputter-coated with Au–Pd and observed using a FE-SEM (Quanta FEG 650 from FEI, Hillsboro, OR) and images were taken at different magnifications.

Hardness and Young's modulus were measured using an MTS NanoIndenter XP having a Berkovich diamond tip with a nominal radius of 50 nm. Tip calibration was performed on the fused silica standard (an accepted Young's modulus of 72 GPa) before and after testing all PTFE samples. All indents, including those on silica, were made to a maximum load of 1.5 mN. The measured Young's modulus and hardness values were determined at the maximum load. Young's modulus of the silica before and after testing the PTFE surfaces was 71.9 ± 1.0 GPa and 72.0 ± 3.0 GPa, respectively. Therefore, moduli from the silica standard did not vary by more than 6%. 15 indents were made on each sample for statistical analysis.

2.3. Cell culture conditions

Human aortic endothelial cells (HAECs) were purchased from Lonza, Inc and cultured in Endothelial Growth Media (EGM-2 BulletKit; Lonza, Walkersville, MD). HAECs were grown to 70–80% confluence under normal cell culture conditions (37 °C, 95% humidity, 5% CO_2) before being seeded onto PTFE sheets.

2.4. MTS assay on PTFE sheets

Samples were prepared by cutting PTFE sheets into circles with diameters of 6.4 mm with various durations of plasma treatment and then sterilizing them with UV light for 3 hours. The sterile samples were then placed into a 96-well plate. 9000 HAEC cells in 200 μL of media were seeded onto each sheet and cultured in an incubator at 37 °C. After culture, an MTS [3-(4,5-dimethylthiazol-2-yl)-5-(3-carboxymethoxyphenyl)-2-(4-sulfophenyl)-2*H*-tetrazolium] assay (CellTiter 96 solution, Promega Co.) was performed to quantify HAEC proliferation on the sheets at 1, 3, and 5 days. HAEC proliferation was assessed on 5 PTFE sheets for each duration of plasma treatment.

2.5. Live/dead assay on PTFE sheets

Samples were prepared by cutting the PTFE sheets into circles with diameters of 9.5 mm and then they were UV sterilized for 3 hours. The samples were then placed into 48-well plates and 25 000 HAEC cells in 400 μL of media were seeded onto each sheet. The cells were cultured at 37 °C for 3 days. After 3 days of culture, viable cells on the sheets were stained by conducting a live/dead viability assay (Molecular Probes Inc., OR). Stained cells were imaged using a Nikon fluorescent microscope and ImageJ software.

2.6. Human platelet adhesion on PTFE sheets

Samples were prepared similarly to those prepared for the live/dead assay and placed in 48-well plates. Platelets (Innovative Research, Inc.) were diluted with Tyrode's solution to a concentration of 6×10^8 platelets per mL. Platelets were then seeded onto the sheets and allowed to incubate for 30 minutes. The sheets were then removed from the plate and washed with PBS to remove free floating platelets. After staining the sheets with calcein AM solution, platelets were visualized with a Nikon fluorescent microscope and ImageJ software.

2.7. SEM imaging for PTFE sheets

Samples were prepared similarly to those prepared for the live/dead assay and placed in 48-well plates. 25 000 HAEC cells in 400 μL of media were seeded onto each sheet and the cells were cultured at 37 °C for 3 days. After culture, the cells were fixed with paraformaldehyde. The fixed samples were dehydrated with ethanol. The PTFE sheets were imaged using a QuantaTM 650 FEG (FEI Co.) with an accelerating voltage of 10 kV.

2.8. Cytoskeletal staining

Samples of the material were prepared and cells were cultured as described for the live/dead analysis. Post culture samples were washed with PBS (1×, 5 min); fixed with paraformaldehyde (4%, 20 min); washed with additional PBS (1×, 5 min), adding Triton X-100 (0.1%). Staining was conducted with 200 μL of the staining solution (PBS 1×, BSA 1%, DAPI 0.1 μg mL^{-1}), the phalloidin–rhodamine conjugate (Abcam, 1× conc.), under dark conditions for 40 min. Then, the samples were rinsed with PBS (1×, 5 min) and the cover slips were added before imaging with a Nikon fluorescent microscope and ImageJ to process the data.

2.9. Statistical analysis

The number of specimens tested for each group was 5 (n = 5). The obtained data in the present study were tested for statistical significance using the ANOVA method (Using the GraphPad Prism software) and $p \leq 0.05$ was defined as significant.

3. Results and discussion

Plasma polymerization is a phenomenon in which vapors of an organic monomer undergo a series of chemical reactions in the plasma phase such as hydrolysis and condensation and get polymerized. TEOS is one such monomer which can undergo plasma polymerization *via* the hydrolysis and condensation reactions. The silica polymerization is usually accomplished *via* a sol–gel reaction in wet chemistry methods. However, plasma based polymerization does not require the use of any bases, solvents and high temperature. Hence, it is a far greener method in comparison with the conventional sol–gel method. In the current work, we have used the plasma polymerization capability of TEOS to polymerize and modify the surface

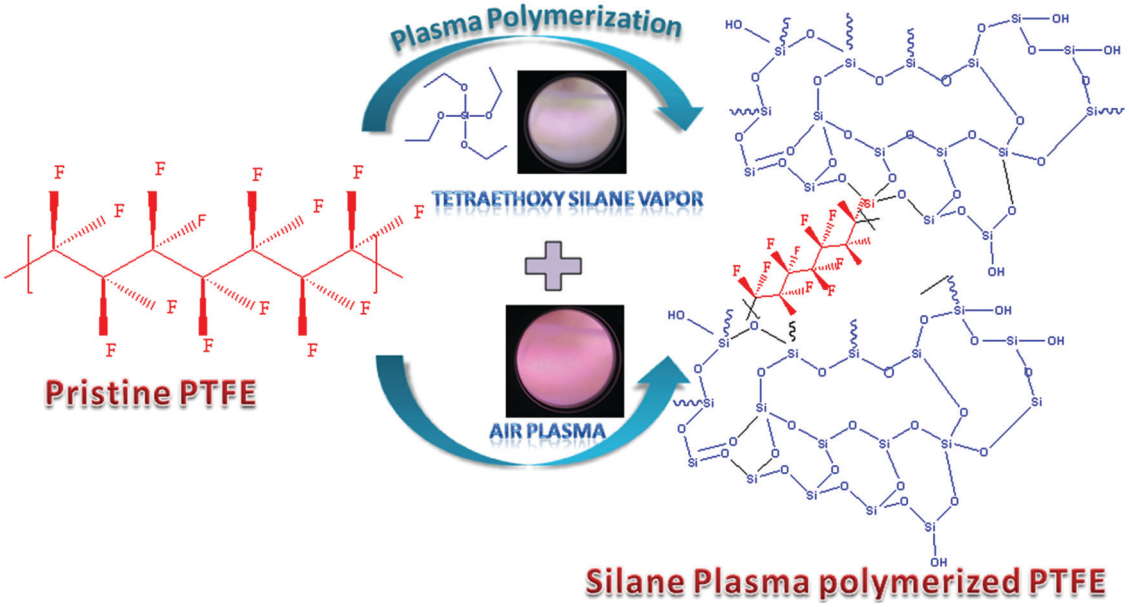

Scheme 1 Schematic representation of the silane plasma polymerization process taking place on the surface of PTFE.

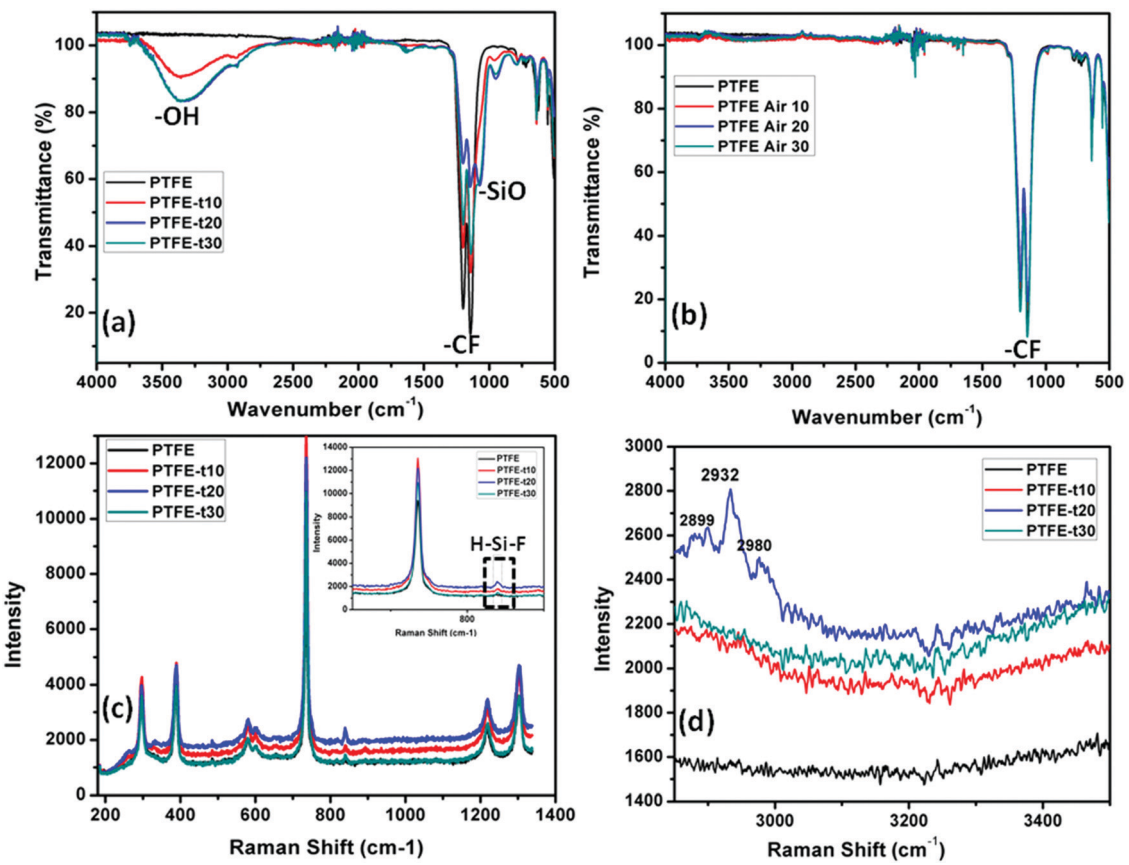

Fig. 1 FTIR spectral analysis of the pristine PTFE, PTFE-t10, PTFE-t20 and PTFE-t30 surfaces (a), comparison of pristine PTFE, PTFE-air 10, PTFE-air 20 and PTFE-air 30 surfaces (b), Raman spectral analysis of the pristine PTFE, PTFE-t10, PTFE-t20 and PTFE-t30 surfaces in the spectral range 180–1350 cm^{-1} (the inset of the graph represents the magnified spectral region from 650–900 cm^{-1}) (c), Raman spectral analysis of the pristine PTFE, PTFE-t10, PTFE-t20 and PTFE-t30 surfaces in the spectral range 2800–3500 cm^{-1} (d).

properties of PTFE, which is a widely used vascular graft material. Air plasma was combined with the vapors of TEOS to facilitate the necessary hydrolysis and condensation reactions to form a plasma polymerized silane coating over the surface of PTFE (Scheme 1). To optimize our process of surface modification of PTFE with the silane derivative, we have comprehensively assessed the influence of the polymerization time over the surface of PTFE. More specifically, we have used different time intervals such as 10, 20 and 30 min of plasma polymerization of TEOS over PTFE. These 3 different plasma polymerized PTFE batches are referred to as PTFE-t10, PTFE-t20 and PTFE-t30 respectively. FTIR spectral comparison of pristine PTFE with PTFE-t10, PTFE-t20 and PTFE-t30 has clearly shown additional bands specifically at 3420 cm^{-1} (attributed to the OH stretching vibrations of the polymerized silane derivatives), 1068 cm^{-1} (attributed to the Si–O stretching vibrations of the polymerized silane derivatives) (Fig. 1a). More specifically, PTFE-t10 and PTFE-t20 exhibit a clear peak that emerges in the region of Si–O stretching vibrations. This suggested the plasma polymerization of silane over the surface of PTFE. The pristine PTFE only exhibited the characteristic stretching vibrations of $-CF_2$ at 1153 cm^{-1} and 1210 cm^{-1} and rolling vibrations of $-CF_2$ groups at 635 cm^{-1}. This clearly supported our hypothesis that the possible plasma polymerization of the TEOS occurred over the surface of PTFE. In order to validate this point, as a control experiment we have also performed the surface modification of PTFE using air (an ambient atmosphere such as feed gas) plasma alone at similar time points. We observed similar bands for both pristine and air plasma modified PTFE in the FTIR spectrum (Fig. 1b). This clearly indicates that air plasma alone cannot impart any significant functionalization on the PTFE surface. Also, it was clear that combining TEOS vapors

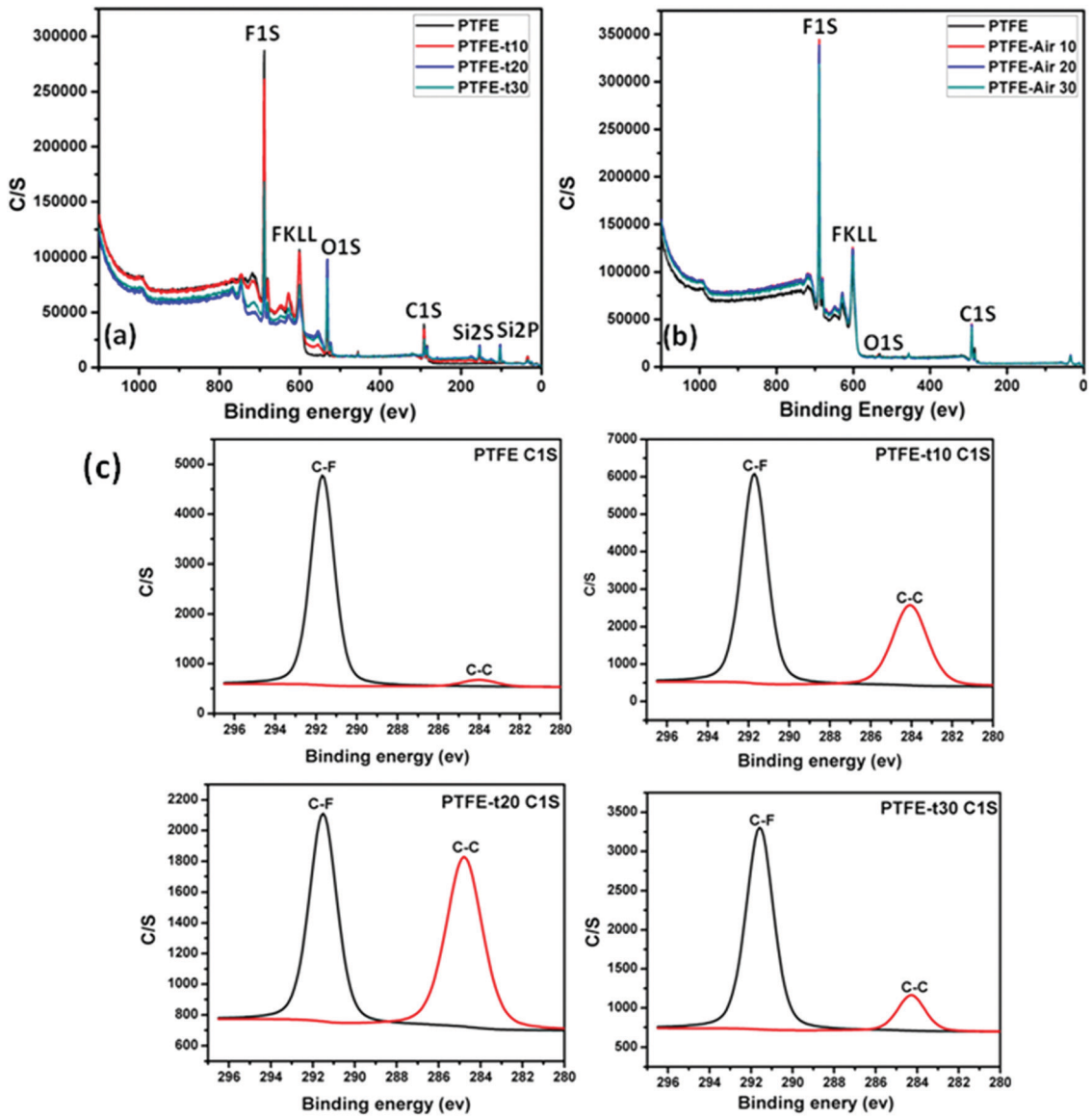

Fig. 2 XPS comparison of the pristine PTFE, PTFE-t10, PTFE-t20 and PTFE-t30 surfaces (a), comparison of pristine PTFE and air plasma modified PTFE at different time periods (b), high resolution C1s XPS spectrum of pristine PTFE, PTFE-t10, PTFE-t20 and PTFE-t30 surfaces (c).

with air plasma resulted in the plasma assisted polymerization of TEOS and subsequent deposition/modification of PTFE surfaces. Hence, taken together the FTIR spectral data clearly suggest the possible plasma polymerization and further modification of the silane derivative on PTFE. Furthermore, we have employed another complementary technique to FTIR specifically, Raman spectral analysis, for the PTFE-t10, PTFE-t20 and PTFE-t30. Raman spectra have shown similar bands for both pristine PTFE and PTFE-t10, PTFE-t20 and PTFE-t30 surfaces, interestingly, it was found that there was a clear peak emerging at 854 cm^{-1} for the PTFE-t10, PTFE-t20 and PTFE-t30 in comparison with the pristine PTFE. This peak at 854 cm^{-1} can be assigned to hydrogen associated with silicon fluoride (H–Si–F) modes.[34] During the process of plasma polymerization of silane, the surface of the fluorinated polymer PTFE can get attached with the silicon and hydrogen atoms of the silane precursor (TEOS) to form H–Si–F type linkages on the surface. This process is expected to be time dependent; hence the corresponding peak also emerged more predominantly with respect to the plasma polymerization time (Fig. 1c). New additional peaks were also present at 2899, 2932 and 2980 cm^{-1} (attributed to the –CH stretching vibrations) for the PTFE-t20 in comparison with pristine PTFE (Fig. 1d). It was worthy of note that PTFE-t10 and PTFE-t20 show the most predominantly emerged additional peaks in this region. Hence, both the FTIR and Raman spectra together suggested the successful silane plasma polymerization process on PTFE. Furthermore, we studied the surface chemistry changes taking place during the plasma polymerization process using the XPS. The XPS spectra of the PTFE-t10, PTFE-t20 and PTFE-t30 surfaces clearly show the presence of silica and surface oxygen (Fig. 2a). The oxygen and silica atomic percentages over the surface have depicted a time dependent behavior with respect to the plasma polymerization time. More specifically, the amount of both oxygen and silica increased when the polymerization time was increased from 10 to 20 min and afterwards it started decreasing at 30 minutes (Table S1, ESI†). This can be attributed to the fact that the plasma polymerization process of TEOS on a short time scale progresses well, and after reaching a point it gets saturated, then reaches equilibrium. This is followed by the phenomenon of surface etching that can reduce the polymerization products through ablation. The control experimental set (air plasma modified PTFE surfaces) has not shown any significant changes in the elemental composition or the presence of silica or a higher oxygen content with respect to the pristine PTFE (Fig. 2b). The high resolution C1s spectrum of pristine PTFE shows two important peaks at 291 eV (attributed to the C–F bonds) and 284 eV (attributed to the C–C bonds present in the surface) (Fig. 2c). Interestingly, the PTFE-t10, PTFE-t20 and PTFE-t30 were clearly exhibiting an increased percentage of the C–C bonds with respect to time.

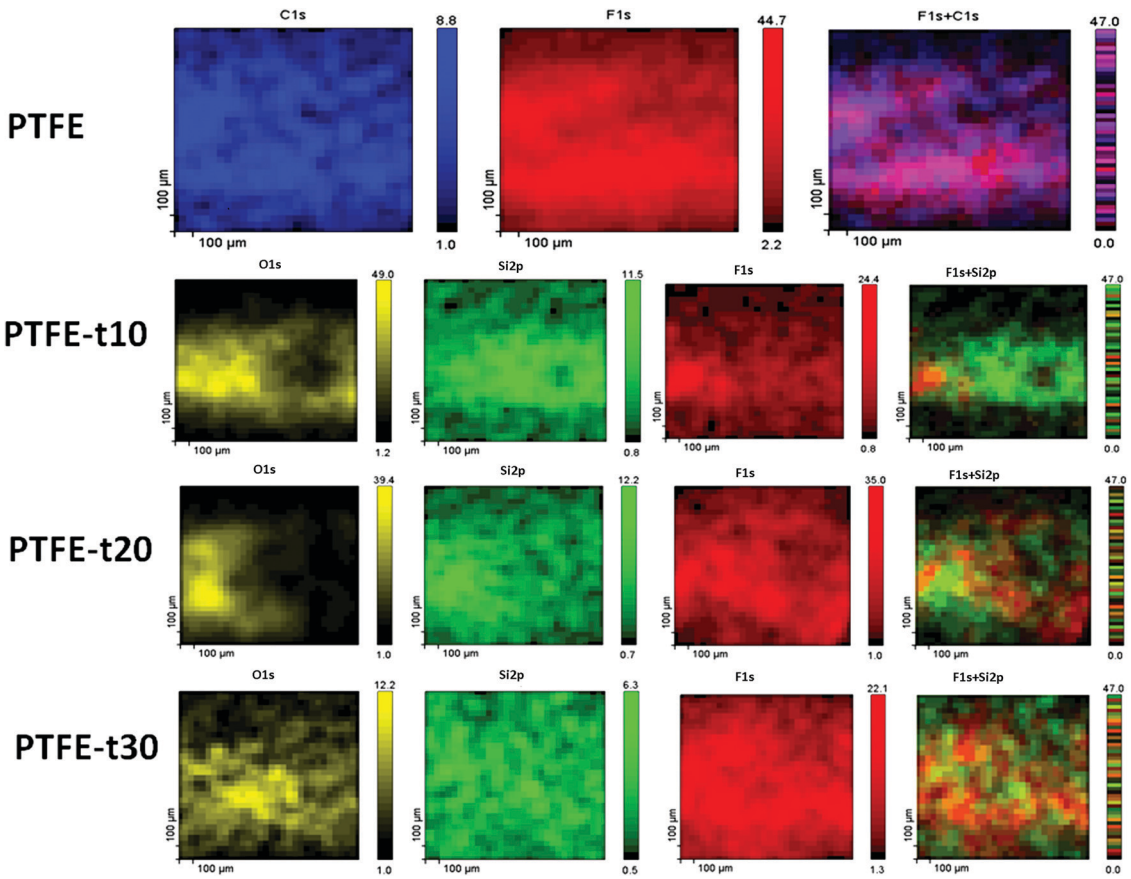

Fig. 3 XPS chemical mapping images of the pristine PTFE, PTFE-t10, PTFE-t20 and PTFE-t30 surfaces.

More specifically, an increase in the C–C bond percentage was observed for PTFE-t10 and PTFE-t20 while for PTFE-t30 that was found to decrease. Thus, the XPS spectra also support the successful silane plasma polymerization process over PTFE. Furthermore, we have carried out the XPS surface chemical mapping for PTFE, PTFE-t10, PTFE-t20 and PTFE-t30. The chemical map of pristine PTFE shows the presence of carbon and fluorine only on the surface. The surface mapping images of PTFE-t10, PTFE-t20 and PTFE-t30 clearly show the additional presence of oxygen (from TEOS) and silica (from TEOS) (Fig. 3). Hence, the surface chemical mapping has strongly suggested the plasma polymerization and subsequent deposition of a silane layer on PTFE surface. Furthermore, we have systematically evaluated the water contact angle on PTFE, PTFE-t10, PTFE-t20 and PTFE-t30. There was a drastic reduction in the water contact angles of the PTFE-t10, PTFE-t20 and PTFE-t30 surfaces in comparison with that of the pristine PTFE (Fig. 4a). More specifically, with water contact angles of $102^\circ \pm 1.23$ (for pristine PTFE), $25^\circ \pm 1.54$ (for PTFE-t10), $61^\circ \pm 1.76$ (for PTFE-t20) and $64^\circ \pm 2.01$ (for PTFE-t30). The wettability measurements suggested that PTFE-t10 produced the most hydrophilic surface modification. The observed high hydrophilicity of the PTFE-t10 may be attributed to the presence of multiple numbers of surface hydroxyl groups that are generated through the plasma polymerization process. However, after reaching saturation, the surface etching phenomenon predominates the surface coating process, this may increase the surface roughness thereby increasing the hydrophobic behavior at longer plasma exposure times. XRD analysis was performed to study the effect of plasma polymerization on the crystalline behavior of PTFE. It was found that both pristine PTFE and PTFE-t10, PTFE-t20 and PTFE-t30 exhibited highly crystalline behavior with a narrow peak at 2θ 18.018° (100 plane) (Fig. 4b). However, upon closely looking this characteristic peak, it was found that the peak position slowly increased for the PTFE-t10 and PTFE-t20 (18.084° & 18.17°) (Fig. 4c). The PTFE-t30 has shown a slight decrease in the peak position compared to that of pristine PTFE, 17.87°. This observed trend can be attributed to the fact that the plasma polymerization/deposition can induce strain in the crystal lattice during the silane coating process. This may be the reason for the observed peak shift from the pristine PTFE. However, for the PTFE-t30, the surface etching becomes more predominant and the strain in the lattice offered by the polymerized layer may have decreased rapidly, this may be the reason for the observed peak shift towards lower values. We hypothesized that the plasma polymerization of the silane precursor and the subsequent coating will reduce the surface roughness of PTFE and will make the

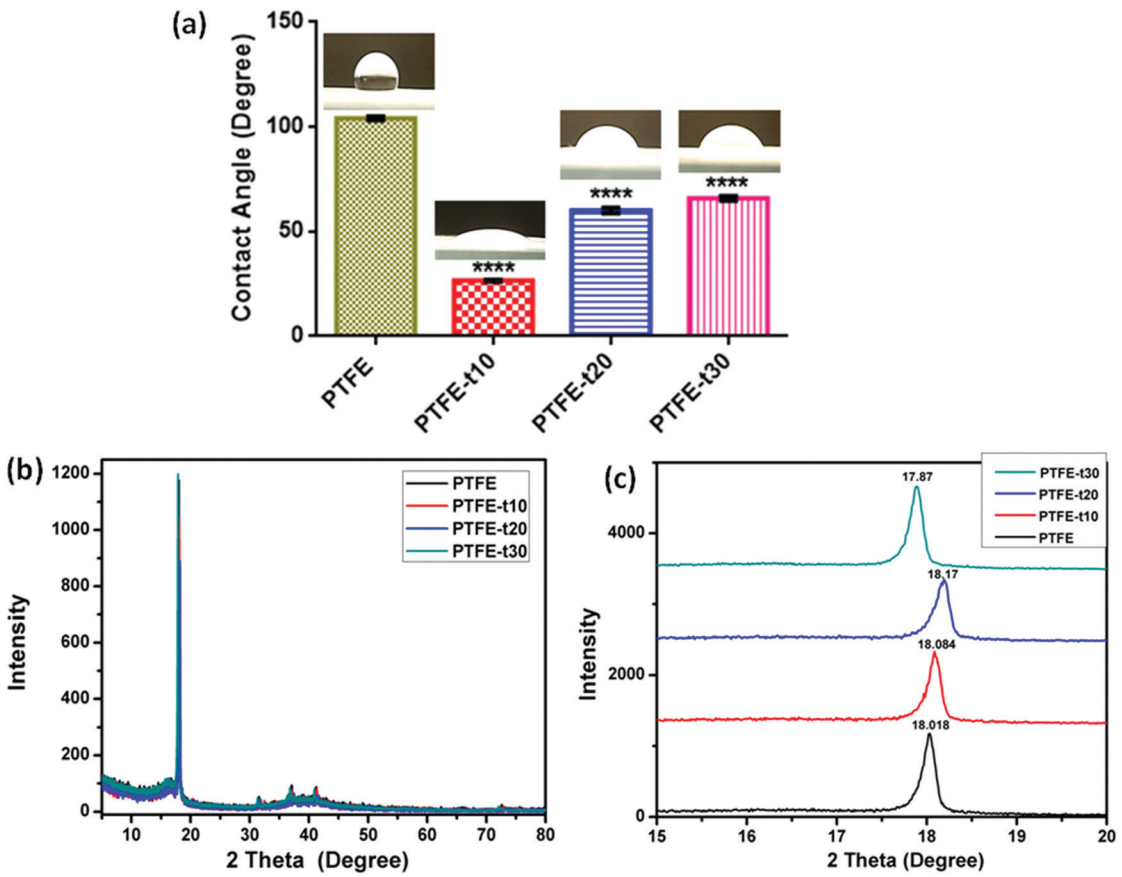

Fig. 4 Contact angle measurements of pristine PTFE, PTFE-t10, PTFE-t20 and PTFE-t30 surfaces (a), X ray diffraction experiments on pristine PTFE, PTFE-t10, PTFE-t20 and PTFE-t30 surfaces (b), magnified X ray diffraction spectra (2θ ranging 15–20°) on pristine PTFE, PTFE-t10, PTFE-t20 and PTFE-t30 surfaces (c).

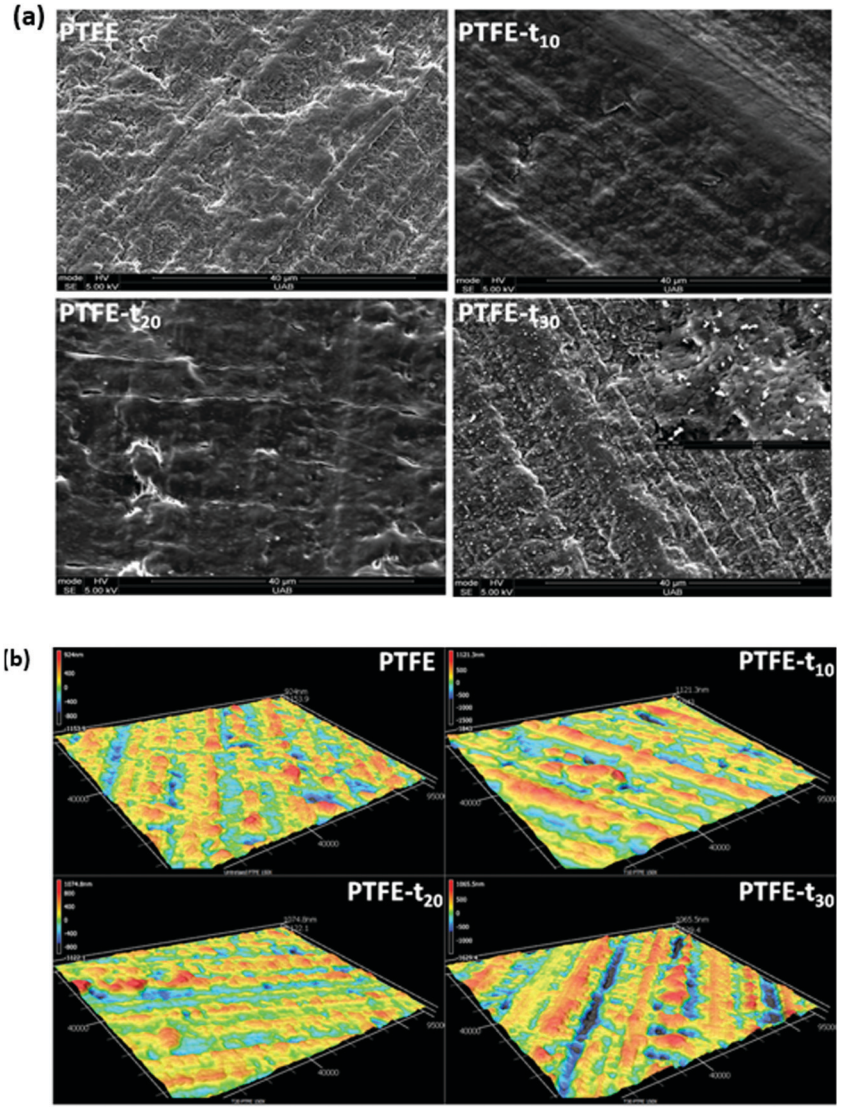

Fig. 5 Scanning electron microscopy of pristine PTFE, PTFE-t10, PTFE-t20 and PTFE-t30 surfaces (a), 3D laser scanning confocal microscopy images of the pristine PTFE, PTFE-t10, PTFE-t20 and PTFE-t30 surfaces (b).

surface more smooth making it favorable for endothelial cell adhesion and proliferation. In order to validate this hypothesis, we have employed the scanning electron microscopy evaluation of the surface features on PTFE, PTFE-t10, PTFE-t20 and PTFE-t30. It was found that the pristine PTFE has irregular surface topography with high irregularities and roughness. The PTFE-t10, and PTFE-t20 surfaces were clearly exhibiting smoother surface topography with much less surface irregularities and roughness (Fig. 5a). During a longer plasma exposure time, along with the deposition of the polymerized layer, the process of surface etching from the plasma becomes predominant. This was clearly visualized for PTFE-t30 where the surface etching of the plasma polymerized layer and the etched coating can be clearly visualized on the surface. This observation was consistent with respect to the XPS results, which show that this process of plasma polymerization after reaching a threshold for PTFE-t20 got reduced significantly and destabilized or surface etching occurs for PTFE-t20, suggesting the possible surface etching phenomenon. The plasma polymerized surface coating was clearly visualized by comparing two different regions in PTFE (one with coating and the other one without any plasma coating). It was seen that the region which was exposed to plasma polymerization clearly exhibits a coated surface compared to the region unexposed to plasma polymerization (Fig. S2, ESI†). The inferences drawn from the SEM imaging were further supported by the 3D laser scanning confocal microscopy results (Fig. 5b). It was seen that for PTFE-t30, the surface was clearly having significant height differences which indicate that potential surface etching took place. Taken together, the SEM and laser scanning microscopy show that plasma polymerization has resulted in the deposition of a silane polymerized layer over PTFE. It was also found that this modification is more stable for PTFE-t10 and PTFE-t20 in comparison with PTFE-t30. The surface mechanical properties of PTFE are relevant to consider for various biomedical applications.

Hence, we have compared the surface mechanics on PTFE-t10, PTFE-t20 and PTFE-t30 at different time points through nanoindentation studies (Fig. 6a). The surface modulus and hardness exhibited by the pristine PTFE sheets were consistent with respect to the previously reported values for PTFE.[35] Furthermore, the nanoindentation studies indicate that the PTFE-t20 and PTFE-t30 have increased Young's modulus and hardness in comparison with those of pristine PTFE and PTFE-T10. The load/displacement curves (Fig. 6a) confirm the plastic depth of indentation to decrease significantly from as high as 57% for the pristine PTFE and PTFE-T10 samples to as low as 34% for the PTFE-T30 sample. The modulus and hardness results are summarized in Fig. 6b, c and in Table S3 (ESI†). Hence, it was clear that this plasma polymerized silane coating not only contributed in making the PTFE surface hydrophilic but also improved the surface mechanical properties of the PTFE, depending on the polymerization time. It is noteworthy that PTFE and PTFE-T10 have exhibited no significant change in the elastic modulus or hardness due to thin-layer surface polymerization. This could be beneficial for their use in cardiovascular applications for which flexibility of a vascular graft with systolic and diastolic pressures is needed.

Thrombosis and poor endothelial cell attachment are some of the major drawbacks for PTFE in blood contact applications. We hypothesized that our modified surfaces with both a high surface oxygen content and high hydrophilicity could address these existing challenges. In order to validate this hypothesis, we studied endothelial cell behaviors of PTFE, PTFE-t10, PTFE-t20. First, we conducted the live/dead cell assay and the PTFE-t10 and PTFE-t20 exhibited a higher number of live endothelial cells than those of the pristine PTFE at 3 days (Fig. 7a). Next, to obtain quantitative information on the proliferation of the endothelial cells on the plasma polymerized PTFE surfaces, we performed the MTS assay for different time points such as 1, 3 and 5 days (Fig. 7b). The PTFE-t10 and PTFE-t20 showed significantly higher endothelial cell proliferation than the pristine PTFE group at 3 and 5 days. Platelet adhesion studies were further carried out to assess the thrombogenicity of the plasma polymerized PTFE surfaces. Interestingly, the PTFE-t10 and PTFE-t20 have shown significantly less adhesion of platelets compared to the pristine PTFE surfaces (Fig. 7c). Thus the platelet adhesion studies suggest the potential non thrombogenicity of the PTFE-t10 and PTFE-t20 surfaces. Albumin is the

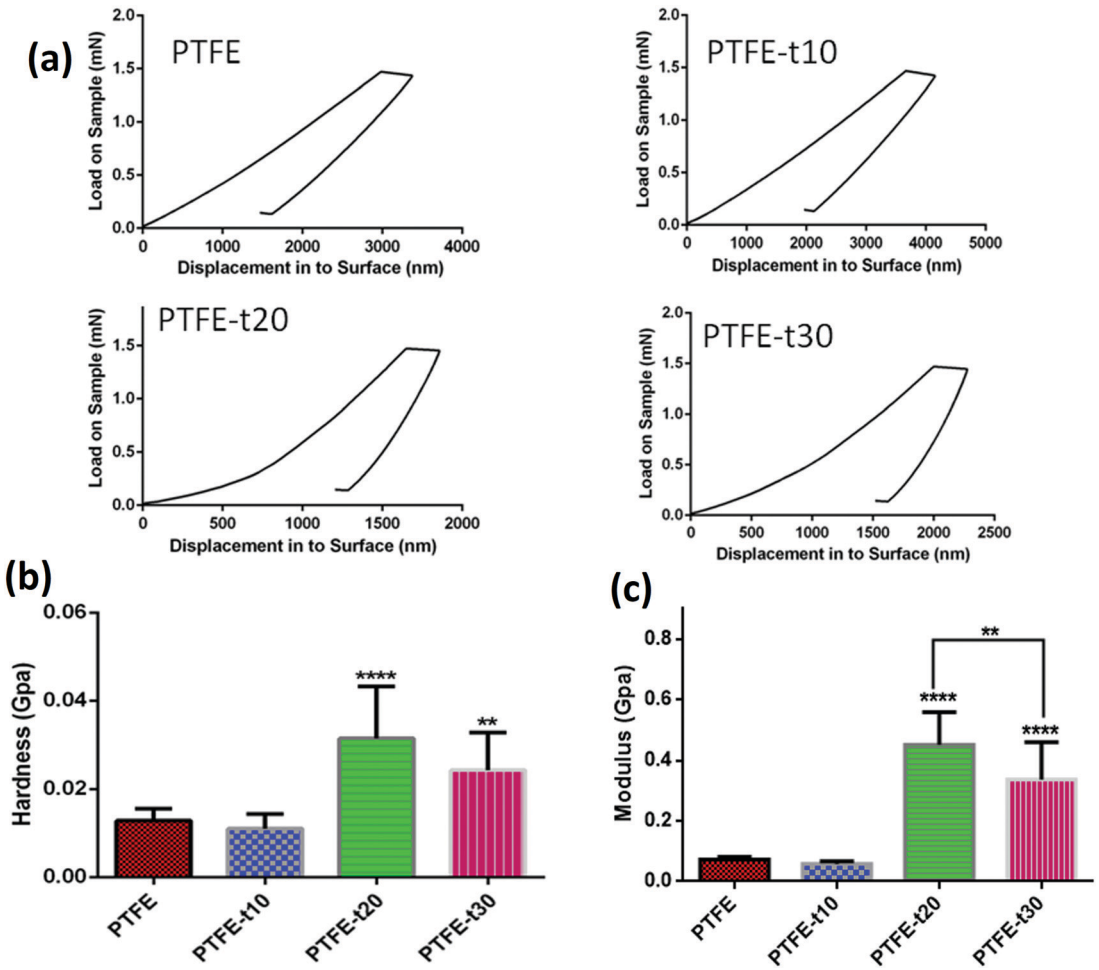

Fig. 6 Nanoindendation studies on pristine PTFE, PTFE-t10, PTFE-t20 and PTFE-t30 surfaces (a), hardness comparison on pristine PTFE, PTFE-t10, PTFE-t20 and PTFE-t30 surfaces (b) and elastic modulus comparison on pristine PTFE, PTFE-t10, PTFE-t20 and PTFE-t30 surfaces (c).

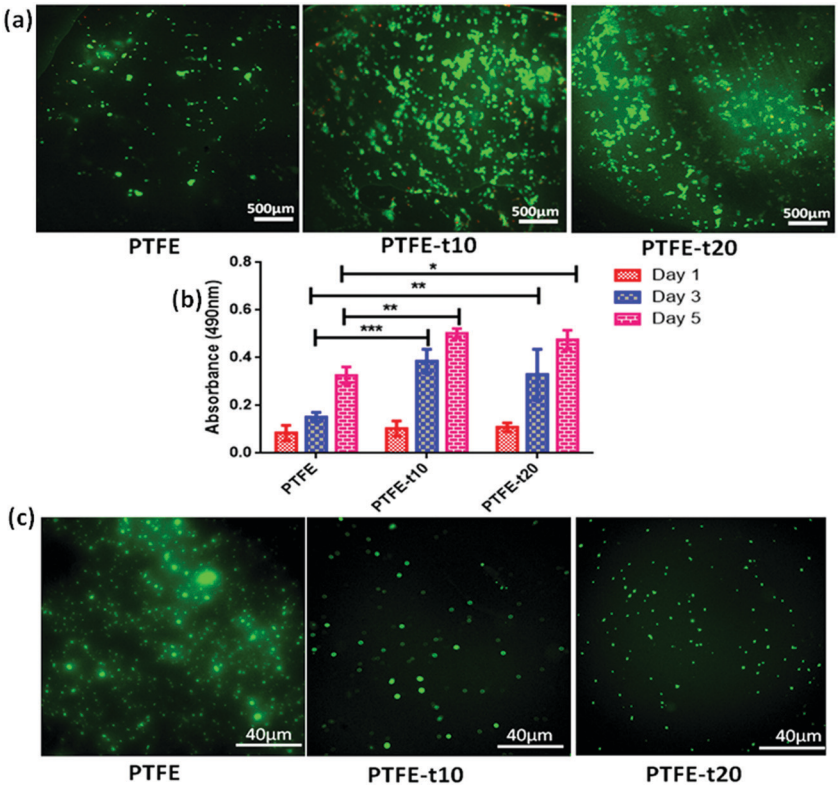

Fig. 7 Live/dead assay on pristine PTFE, PTFE-t10 and PTFE-t20 surfaces after 3 days of endothelial cell seeding (a), MTS assay on pristine PTFE, PTFE-t10 and PTFE-t20 surfaces after 1, 3 and 5 days of endothelial cell seeding (b) platelet adhesion studies on pristine PTFE, PTFE-t10 and PTFE-t20 surfaces (c).

most abundant protein in the blood plasma which when adsorbed on the surface of vascular prosthesis found to reduce the nonspecific protein adsorption cascades and reduce the thrombosis.[36] Hence, we have performed a preliminary qualitative albumin adsorption study on PTFE-t10. More specifically FITC tagged bovine serum albumin (BSA) protein adsorption studies were done to compare the albumin adsorption between pristine PTFE and PTFE-t10. Very bright fluorescence was observed from PTFE-t10 in comparison with pristine PTFE surfaces (Fig. S4a, ESI†). This clearly suggest the higher albumin adsorption on PTFE-t10. This may be the reason for the observed low platelet adhesion of the PTFE-t10 in comparison with the pristine PTFE surfaces. The observed higher BSA adsorption also supported the higher endothelial cell proliferation on PTFE-t10. Polymers like polyethylene glycol (PEG) were found to exhibit similar antifouling properties due to a number of factors such as the steric effect, hydration and chain mobility.[37] We hypothesize that the observed trend of low platelet adhesion on PTFE-t10 and PTFE-t20 surfaces can also be attributed to the similar effects which can be offered by the random silane polymer chains such as the steric effect, hydration (due to a very high number of surface hydroxyl groups) and random polymer chains (which are a hallmark of the plasma polymerization process).

SEM imaging of the fixed endothelial cells on PTFE-t10, PTFE-t20 and pristine PTFE surfaces also showed a drastic difference in their morphology. Interestingly, the 10 min plasma polymerized PTFE surface has clearly showed more spreaded endothelial cells with formation of pseudopods when compared to the pristine PTFE (Fig. S4b, ESI†). We also observed a similar trend of cell adhesion through the phalloidin cytoskeleton staining. The plasma polymerized PTFE surfaces exhibited cell sprouting and the images showed an extended cytoskeleton when compared to the pristine PTFE (Fig. 8). The observed higher endothelial proliferation and

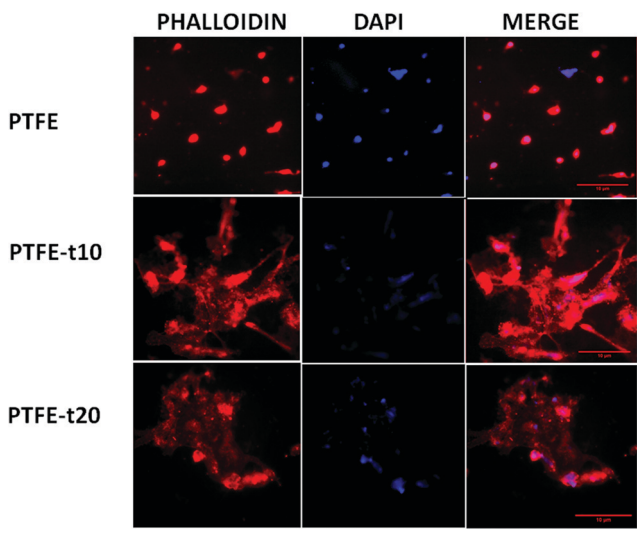

Fig. 8 Rhodamine phalloidin cytoskelton staining on pristine PTFE, PTFE-t10 and PTFE-t20 surfaces after 3 days of endothelial cell seeding.

cytoskeleton spreading on PTFE-t10 and PTFE-t20 can be attributed to a number of factors such as a very high surface oxygen content, high hydrophilicity and a smooth surface (offered by the coating). Taken together, the endothelial cell proliferation and platelet adhesion studies suggested that the PTFE-t10 and PTFE-t20 surfaces were found to exhibit good endothelial cell adhesion with low platelet adhesion. The observed phenomenon of low platelet adhesion and higher endothelial cell proliferation was consistent with the previously reported chondroitin sulfate coating on PET surfaces for vascular implants.[38] This study attributed the higher endothelial cell adhesion to the presence of the negatively charged surface chondroitin sulfate coating which can selectively adsorb fetal bovine serum (FBS) proteins or growth factors. We hypothesize that our present plasma polymerized silane coating having very high number of surface hydroxyl groups can bind selectively to FBS proteins similar to that of the chondroitin sulfate coating that can facilitate more endothelialization.

4. Conclusions

In conclusion, we report a new facile organosilane plasma polymerization method to tailor the surface properties of PTFE. We hypothesized that the plasma polymerization of silane can augment the PTFE surface properties with characteristics such as high hydrophilicity, a high surface oxygen content and improved endothelial cell adhesion. This hypothesis was clearly justified by the material and biological characterization performed on the plasma modified PTFE surfaces. The results of different techniques such as FTIR, XPS, XRD and SEM have clearly proved the successful plasma polymerization and subsequent coating of hydrophilic thin layers on the surface of PTFE. The endothelial cell proliferation and platelet adhesion studies have shown that the plasma polymerized PTFE surfaces favored good endothelial cell adhesion with minimal platelet adhesion. More importantly, the reported method was a facile single step surface modification technique which does not require any further post modification steps to augment PTFE surfaces with better endothelial cell adhesion and reduced platelet adhesion. Taken together, these results suggest the potential of this methodology towards potential blood contact applications.

Conflicts of interest

There are no conflicts to declare.

Acknowledgements

This work was supported by funding through NSF EPSCoR RII-Track-1 Cooperative Agreement OIA-1655280. We also acknowledge the NSF Major Research Instrumentation (MRI) Grant No. DMR-1725016 for XRD facility. HWJ and PTH acknowledge the partial support from NIH 1R01HL125391-01 and NIH 2R44DK109789-02. BT acknowledges the fellowship from Department of Education GAANN Grant No. P200A180001. V. M. V. expresses special thanks to Dr Paul Baker for assistance in XPS and XRD analyses. Any statement, opinion, recommendation, or conclusions shared are those only of the authors and do not necessary relay the official positions of the National Science Foundation or the US Department of Education.

References

1 C. Oehr, *Nucl. Instrum. Methods Phys. Res., Sect. B*, 2003, **208**, 40–47.
2 D. L. Elbert and J. A. Hubbell, *Annu. Rev. Mater. Sci.*, 1996, **26**, 365–394.
3 P. Chu, *Mater. Sci. Eng., R*, 2002, **36**, 143–206.
4 R. N. S. Sodhi, *J. Electron Spectrosc. Relat. Phenom.*, 1996, **81**, 269–284.
5 R. Landgraf, M.-K. Kaiser, J. Posseckardt, B. Adolphi and W.-J. Fischer, *Procedia Chem.*, 2009, **1**, 1015–1018.
6 B. R. Coad, T. Scholz, K. Vasilev, J. D. Hayball, R. D. Short and H. J. Griesser, *ACS Appl. Mater. Interfaces*, 2012, **4**, 2455–2463.
7 K. S. Siow, L. Britcher, S. Kumar and H. J. Griesser, *Plasma Processes Polym.*, 2006, **3**, 392–418.
8 H. S. Sundaram, X. Han, A. K. Nowinski, N. D. Brault, Y. Li, J.-R. Ella-Menye, K. A. Amoaka, K. E. Cook, P. Marek, K. Senecal and S. Jiang, *Adv. Mater. Interfaces*, 2014, **1**, 1400071.
9 A. A. John, A. P. Subramanian, M. V. Vellayappan, A. Balaji, S. K. Jaganathan, H. Mohandas, T. Paramalinggam, E. Supriyanto and M. Yusof, *RSC Adv.*, 2015, **5**, 39232–39244.
10 A. Vesel and M. Mozetic, *Vacuum*, 2012, **86**, 634–637.
11 P. Chevallier, M. Castonguay, S. Turgeon, N. Dubrulle, D. Mantovani, P. H. McBreen, J.-C. Wittmann and G. Laroche, *J. Phys. Chem. B*, 2001, **105**, 12490–12497.
12 S. B. Idage and S. Badrinarayanan, *Langmuir*, 1998, **14**, 2780–2785.
13 N. Inagaki, S. Tasaka, K. Narushima and K. Teranishi, *J. Appl. Polym. Sci.*, 2002, **83**, 340–348.
14 J. Nakamatsu, L. F. Delgado-Aparicio, R. Da Silva and F. Soberon, *J. Adhes. Sci. Technol.*, 1999, **13**, 753–761.
15 M. Modic, I. Junkar, A. Vesel and M. Mozetic, *Surf. Coat. Technol.*, 2012, **213**, 98–104.
16 M. C. Vasudev, K. D. Anderson, T. J. Bunning, V. V. Tsukruk and R. R. Naik, *ACS Appl. Mater. Interfaces*, 2013, **5**, 3983–3994.
17 F. Khelifa, S. Ershov, Y. Habibi, R. Snyders and P. Dubois, *Chem. Rev.*, 2016, **116**, 3975–4005.
18 A. Michelmore, J. D. Whittle, R. D. Short, R. W. Boswell and C. Charles, *Plasma Processes. Polym.*, 2014, **11**, 833–841.
19 G. Aziz, R. Ghobeira, R. Morent and N. D. Geyter, in *Recent Research in Polymerization*, ed. N. Cankaya, InTech, 2018.
20 P. Cools, C. Mota, I. Lorenzo-Moldero, R. Ghobeira, N. De Geyter, L. Moroni and R. Morent, *Sci. Rep.*, 2018, **8**, 3830.
21 R. Bitar, P. Cools, N. De Geyter and R. Morent, *Appl. Surf. Sci.*, 2018, **448**, 168–185.
22 X. Liu, Q. Feng, A. Bachhuka and K. Vasilev, *ACS Appl. Mater. Interfaces*, 2014, **6**, 9733–9741.

23 P. Cools, H. Declercq, N. De Geyter and R. Morent, *Appl. Surf. Sci.*, 2018, **432**, 214–223.
24 S. Roll, J. Müller-Nordhorn, T. Keil, H. Scholz, D. Eidt, W. Greiner and S. N. Willich, *BMC Surg.*, 2008, **8**, 22.
25 E. A. Santiago-Delpin and T. Aviles, *Am. J. Surg.*, 1980, **140**, 315–319.
26 A. G. Nordestgaard, J. A. Buckels and S. E. Wilson, *Br. J. Exp. Pathol.*, 1986, **67**, 839–849.
27 S. Zanini, R. Barni, R. D. Pergola and C. Riccardi, *J. Phys. Appl. Phys.*, 2014, **47**, 325202.
28 S. D. Pringle, V. S. Joss and C. Jones, *Surf. Interface Anal.*, 1996, **24**, 821–829.
29 N. Inagaki, S. Tasaka and T. Umehara, *J. Appl. Polym. Sci.*, 1999, **71**, 2191–2200.
30 J. Nakamatsu, L. F. Delgado-Aparicio, R. Da Silva and F. Soberon, *J. Adhes. Sci. Technol.*, 1999, **13**, 753–761.
31 H.-Y. Mi, X. Jing, J. A. Thomsom and L.-S. Turng, *J. Mater. Chem. B*, 2018, **6**, 3475–3485.
32 B. Cheng, Y. Inoue and K. Ishihara, *Colloids Surf., B*, 2019, **173**, 77–84.
33 B. S. Tucker, P. A. Baker, K. G. Xu, Y. K. Vohra and V. Thomas, *J. Vac. Sci. Technol., A*, 2018, **36**, 04F404.
34 P. G. Spizzirri, J.-H. Fang, S. Rubanov, E. Gauja and S. Prawer, 2010, arXiv:1002.2692.
35 I. C. Halalay, M. J. Lukitsch, M. P. Balogh and C. A. Wong, *J. Power Sources*, 2013, **238**, 469–477.
36 B. Sivaraman and R. A. Latour, *Biomaterials*, 2010, **31**, 1036–1044.
37 L.-C. Xu and C. A. Siedlecki, *J. Biomed. Mater. Res., Part B*, 2017, **105**, 668–678.
38 K. Thalla, H. Fadlallah, B. Liberelle, P. Lequoy, G. De Crescenzo, Y. Merhi and S. Lerouge, *Biomacromolecules*, 2014, **15**, 2512–2520.